Progressive Rearrangement of Subtilisin Carlsberg into Orderly and Inflexible Conformation with Ca^{2+} Binding

Sunbae Lee and Du-Jeon Jang
School of Chemistry and Molecular Engineering, Seoul National University, Seoul 151–742, Korea

ABSTRACT Fluorescence depolarization and decay kinetic profiles, together with differential scanning calorimetric thermograms and circular dichroism spectra, are measured to understand the respective roles of Ca^{2+} ions at the strong (Ca1) and weak binding sites (Ca2) of subtilisin Carlsberg (sC). Thermal denaturation temperature decreases considerably with Ca1 removal, whereas it does slightly with Ca2 removal. The fraction of random coil structure increases significantly with Ca2 removal as well as with Ca1 removal. sC shows three fluorescence decay times of 100, 1100, and 3300 ps. Although the fast and the slow do not change noticeably, the medium one decreases progressively with Ca^{2+} removal. sC has two fluorescence anisotropic decay components of 340 and 12,000 ps. The fast one arises from the internal rotation of Tyr, whereas the slow results from the global rotation of sC. Although both become significantly faster with Ca2 removal, only the slow one becomes slightly faster with further Ca1 removal. Overall, sC undergoes progressive rearrangement into disorderly and flexible conformation with Ca^{2+} removal, indicating that both Ca1 and Ca2 are indispensable for the stable structure of sC.

INTRODUCTION

Subtilisins comprise a group of serine proteases that are secreted in large amounts from a wide variety of *Bacillus* species. Serine proteases, present in virtually all organisms, exist as two families, the "trypsin-like" and the "subtilisin-like," that have independently evolved a similar catalytic device characterized by the triad of Ser, His, and Asp (Carter and Wells, 1988). Subtilisins are of considerable interest not only scientifically but also industrially, for they are used in such diverse applications as meat tenderizers, laundry detergents, and proteolytic medicines (Genov et al., 1995; Fitzpatrick et al., 1994). Furthermore, their catalytic efficiency and specificity in organic media would enhance practical uses related to synthetic applications (Broos et al., 1995; Chatterjee and Russell, 1993; Chaudhary et al., 1996; Kijima et al., 1994). There have been many researches about their stability (Pantoliano et al., 1989; Siezen et al., 1991; Strausberg et al., 1993) as stabilization normally improves their properties for applications. In many enzymes, metal ions have been reported to play an important role in stabilizing proteins by binding at specific sites (Genov et al., 1995). The additional contribution of four Ca^{2+} binding to thermolysin, a neutral protease having four Ca^{2+} binding sites, is collectively as high as 9 kcal/mol in the free energy of unfolding (Voordouw et al., 1976). Similarly, the binding of Ca^{2+} to the two noncooperative high-affinity sites of parvalbumin III from carp muscle enlarges the overall unfolding free energy by 10.6 kcal/mol and the thermally unfolding transition temperature by 50°C.

Received for publication 27 March 2001 and in final form 27 July 2001.
Address reprint requests to Dr. Du-Jeon Jang, School of Chemistry and Molecular Engineering, Seoul National University, Seoul 151-742, Korea. Tel.: 82-2-875-6624; Fax: 82-2-889-1568; E-mail: djjang@plaza.snu.ac.

0006-3495/01/11/2972/07 $2.00

It is reported (Ghadiri et al., 1992; Handel et al., 1993; Lieberman and Sasaki, 1991) that metal ion binding to the apoprotein of a conjugated protein replaces some of the non-specific interactions with more geometrically restrictive metal-ligand interactions and so drives the polypeptide chain to fold into a unique structure. Metal ion binding is also reported to stabilize the peptide secondary structure of a designed polypeptide by ligating metal ions to negatively charged side chains that would otherwise repel each other (Cheng et al., 1996; Kohn et al., 1998; Schneider and Kelly, 1995; Tian and Bartlett, 1996; Ghadiri and Choi, 1990; Ruan et al., 1990). Thus it is very important to understand the structural and functional roles of metal ion binding sites from the standpoint of industrial applications as well as of academic interest.

Subtilisin Carlsberg (sC), secreted by *Bacillus licheniformis* (Smith et al., 1968), is a single polypeptide chain of 274 amino acid residues with two Ca^{2+} ion binding sites (Bode et al., 1987; McPhalen and James, 1988; Neidhart and Petsko, 1988). The x-ray structure of the strong site with a binding constant of 10^8 (Pantoliano et al., 1989) has an approximately octahedral coordination sphere (Bode et al., 1987; McPhalen and James, 1988; Neidhart and Petsko, 1988), whereas the weak site with a binding constant of 10^2 (Pantoliano et al., 1988) has a quadrangular pyramidal structure (Bode et al., 1987; McPhalen and James, 1988). However, we have suggested (Lee and Jang, 2000) that in solution the Ca^{2+} bound in the strong binding site of sC (Ca1) forms an additional coordination bond to a solvent or substrate molecule. Ca^{2+} binding to sC is known to slow down autolysis and to enhance thermal stability (Pantoliano et al., 1988). The Ca^{2+} binding at the weak site as well as at the strong site of the subtilisin BPN′, which is similar to sC in structure, is reported to enhance the protein stability dramatically (Kidd et al., 1996).

Differential scanning calorimetry (DSC) is often used to monitor the thermally induced unfolding transition of a

protein. The transition temperature, where the endothermic unfolding transition is maximum, provides an approximate measure for the thermal stability of the protein. Near-ultraviolet (UV) circular dichroism (CD) is useful for monitoring the local tertiary structure of a protein in the vicinity of the aromatic residues sensitively. Thus, near-UV CD is particularly useful for probing small changes introduced by chemical modification, ligand binding, or site-directed mutagenesis. On the other hand, far-UV CD is valuable for determining the secondary structural constitution of a protein because the CD spectra of the three secondary structure types are very different from one another in the far-UV region.

Trp and Tyr are responsible for the fluorescence of proteins, and sC has only one Trp and 13 Tyr residues (Smith et al., 1968). Trp fluorescence is known to predominate over Tyr fluorescence, probably due to quenching or energy transfer. An exception is sC, which exhibits Tyr fluorescence dominantly (Kijima et al., 1994; Willis and Szabo, 1989). Tyr contribution becomes negligibly small when sC is excited at or above 295 nm (Grinvald and Steinberg, 1976; Lakowicz et al., 1983; Lakshmikanth and Krishnamoorthy, 1999; Nishimoto et al., 1998). Thus the fluorescence spectra have often been measured with excitation at 295 nm to minimize the complexity arising from Tyr contribution. However, in this study fluorescence is to be collected after exciting Tyr as well as Trp to probe the overall structural changes with Ca^{2+} removal.

We have measured fluorescence depolarization and decay kinetic profiles as well as differential scanning calorimetric thermograms and CD spectra to understand the respective roles of Ca1 and Ca^{2+} bound at the weak binding sites of sC (Ca2). Our results show that the conformation of sC progressively becomes disorderly and flexible with Ca^{2+} removal.

MATERIALS AND METHODS

Trizma ($H_2NC(CH_2OH)_3$) and sC were used as purchased from Sigma (St. Louis, MO). Metal cation-removed sC from the strong binding site as well as from the weak binding site (dSsC) was prepared by equilibrating 0.5 mM sC with 20 mM EDTA for one-half hour in aqueous buffer (pH 7.5) solution of 0.1 M Trizma. Metal-cation removed sC from the weak binding site (dWsC) was prepared by the same procedures as dSsC, except for the EDTA concentration (2 mM). All the samples of dSsC and dWsC as well as native sC (NsC) were prepared just before use to minimize the concentration of autolyzed sC. The concentration of sC was determined by measuring absorbance at 280 nm, where the extinction coefficient is $2.5 \times 10^4\ M^{-1}\ cm^{-1}$ (Genov et al., 1995). All the measurements, except DSC measurements, were performed at room temperature.

DSC measurements were performed using a Thermoflex DSC 8131 (Rigaku, TAS 100) at a scan rate of 2°C per min, whereas CD spectra were collected using a spectropolarimeter (Jasco, J-600).

Fluorescence decay and depolarization kinetics were measured using an actively/passively mode-locked Nd:YAG laser (Quantel, YG501) and a 10-ps streak camera (Hamamatsu, (2830) attached with a CCD detector (RTE128H, Princeton Instruments). The polarized (polarization purity ≥99%) laser pulses of 25 ps, 266 nm, and 1 mJ were focused on a sample with the spot diameter of 2 mm for excitation. Emission was collected at near magic angle (54.7°) and right angle for decay and depolarization measurements, respectively, from sample excitation. Emission wavelength was selected using a combination of band-pass filters for kinetics or a 0.15-m monochromator (Spectrapro 150, Acton Research) for time-resolved spectra. In fluorescence depolarization measurements the emission intensities (I) of the polarizations parallel (∥) and perpendicular (⊥) to the polarization of excitation light were measured independently using both vertically and horizontally polarized laser pulses. Fluorescence anisotropy at time t, $r(t)$, was calculated as

$$r(t) = [I_{\parallel}(t)\ G - I_{\perp}(t)] / [I_{\parallel}(t)G + 2\,I_{\perp}(t)] \qquad (1)$$

in which G is a correction factor for the efficiencies of the detector toward vertically and horizontally polarized light. The G-value is experimentally measured as the ratio of the vertical emission to the horizontal emission when the excitation is horizontally polarized.

Fluorescence decay and depolarization kinetic parameters were extracted by fitting measured kinetic profiles to computer-simulated kinetic curves convoluted with respective instrumental response functions. Fluorescence decay and depolarization kinetics were fitted to

$$I(t) = \sum f_i \exp(-t/\tau_i) \qquad (2)$$

$$r(t) = r_0 \sum \beta_i \exp(-t/\phi_i) \qquad (3)$$

respectively. The f_i and τ_i in Eq. 2 are the initial fractional fluorescence intensity and time constant of each decay component, respectively. On the other hand, r_0 in Eq. 3 is the initial anisotropy and β_i and ϕ_i are the fractional contribution and rotational correlation time, respectively, of each depolarization component. In general, the rotational dynamics of a fluorophore attached in a macromolecular system is deconvoluted into two correlation components, which are the rotational motion of the whole macromolecule and the internal motion of the fluorophore with respect to the macromolecule. As $[I_{\parallel}(t)G + 2I_{\perp}(t)]$ represents the total fluorescence intensity, we have checked whether its decays agree with fluorescence decay profiles measured at near magic angles. Satisfactory agreements were found within experimental errors.

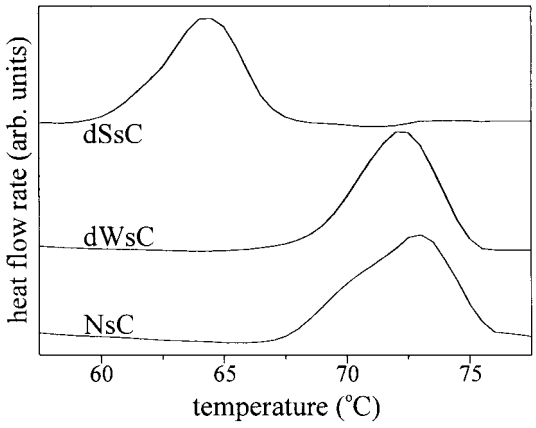

FIGURE 1 DSC thermograms of indicated sC having respective concentrations of 0.5 mM in aqueous buffer (pH 7.5) solutions of 0.1 M Trizma. The estimated denaturation temperatures are 73.0°C for NsC, 72.2°C for dWsC, and 64.3°C for dSsC.

RESULTS AND DISCUSSION

Fig. 1 shows that the thermally induced unfolding transition

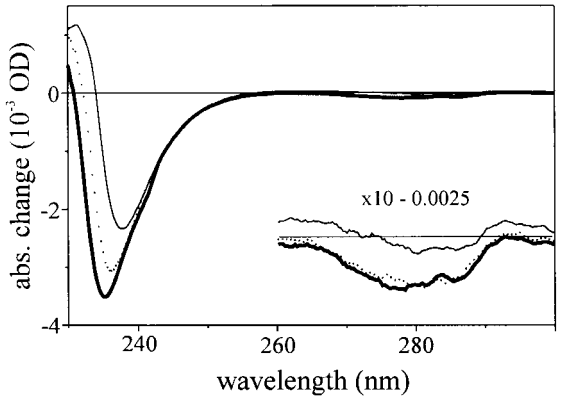

FIGURE 2 CD spectra of NsC (*boldly solid*), dWsC (*dotted*), and dSsC (*thinly solid*) with respective concentrations of 0.5 mM in aqueous buffer (pH 7.5) solutions of 0.1 M Trizma.

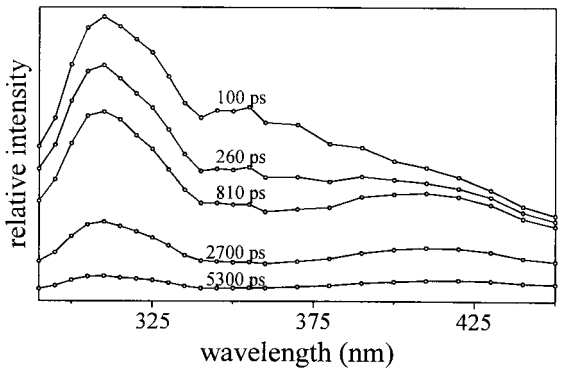

FIGURE 3 Time-resolved fluorescence spectra of 0.8 mM NsC in aqueous buffer (pH 7.5) solution of 0.1 M Trizma at the shown time delays after excitation at 266 nm.

temperature decreases considerably (by 8.7°C) with the removal of both Ca1 and Ca2, whereas it does slightly (by 0.8°C) with the removal of Ca2 only. This indicates that the denaturation temperature increases greatly with Ca1 binding, rather than Ca2 binding. (The shoulder of the DSC thermogram of NsC near 70°C results from the denaturation of autolyzed sC because sC was used as received without further purification. This suggests that the native polypeptide chain having both Ca1 and Ca2 has the highest thermal stability.) Ca1 is crucial for the thermal stability of sC whereas Ca2 is also somewhat helpful. Although the effects of others such as mutation and medium on the thermal stability of subtilisins have been already studied with DSC (Pantoliano et al., 1989; Yang et al., 1996), we are reporting DSC results for the individual effects of Ca1 and Ca2 on the thermal stability of sC for the first time.

Although Ca1 is much more vital to the thermal stability than Ca2, the CD spectra of Fig. 2 suggest that both Ca1 and Ca2 are crucial to the stability of the secondary structures. Absorbance at the absorption minimum of NsC near 235 nm increases sequentially as the fraction of the random coil structure increases progressively with Ca^{2+} removal (Table 1). Far-UV CD spectra below 250 nm are extremely sensitive to the secondary structures of proteins and are useful for estimating the fractional constitution of α-helix, β-sheet, and random coil. The determination of individual secondary structure fractions by analyzing CD spectra has been widely used (Venyaminov and Yang, 1996). Although the fractions of α-helix, β-sheet, turn, and random coil in NsC are reported as 0.31, 0.1, 0.22, and 0.37, respectively, from the x-ray structure (Chang et al., 1978), they are found to be 0.22, 0.47, 0, and 0.31, respectively, from the CD spectrum (Bayley et al., 1989). This indicates that the fractions calculated from CD spectra have large errors inherently. Thus we estimated just the approximate fractional changes of the constituting secondary structures with Ca^{2+} removal, considering the secondary structure fractions of NsC by Bayley et al. (1989) and the basis spectra and estimation method of secondary structures by Saxena and Wetlaufer (1971). Despite large uncertainties, we are showing experimentally for the first time the progressive structural changes of sC with Ca^{2+} binding. Sequential Ca^{2+} binding to the negatively charged side chains of the strong and the weak binding sites, which would otherwise repel each other (Kohn et al., 1998; Schneider and Kelly, 1995), changes the secondary structure constitution and enhances the stability progressively.

TABLE 1 Approximate fractional changes of the secondary structures of Ca^{2+}-removed sC compared with NsC, estimated from Fig. 2

Sample	α-Helix	β-Sheet	Random coil
dWsC	−0.1	−0.1	0.2
dSsC	−0.2	−0.3	0.5

Estimation method is described in the text.

On the other hand, because near-UV CD is particularly sensitive to local tertiary structures in the vicinity of the aromatic residues, it is generally an excellent qualitative indicator for small changes introduced by chemical modification or ligand binding. The near-UV CD band of Fig. 2 is relatively featureless at 280 nm as it results from the superposition of a large number of different Tyr and Trp residues. Nevertheless, the near-UV CD hardly changes with the removal of Ca2 but it does noticeably with the removal of Ca1. This indicates that some chiral aromatic residues of Tyr and Trp near the strong site are subject to local structural changes with Ca1 binding. Considering both DSC and CD measurements, we suggest that both Ca1 and Ca2 are essential for the stable structure of sC, although Ca1 is more crucial to the thermal stability. As Ca1 binds to sC, the enzyme forms a metastable structure, which already has the substantial conformation of sC. However, both Ca1 and Ca2 are suggested to be indispensable for the stable structure of sC.

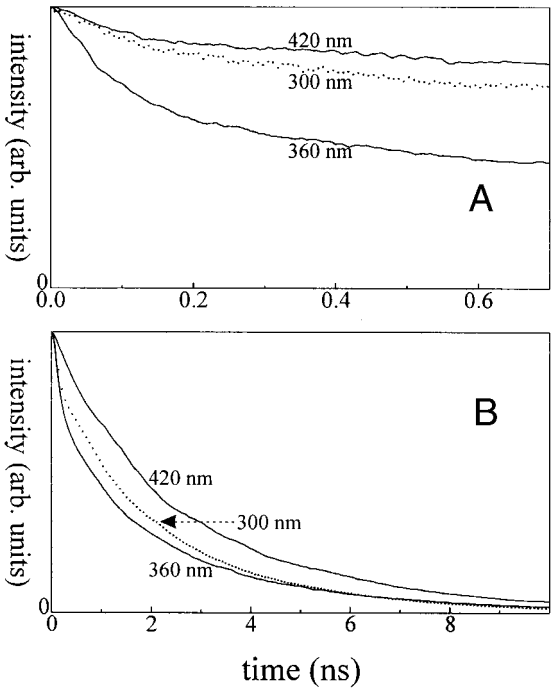

FIGURE 4 Fluorescence kinetic profiles, displayed in short (*a*) and long (*b*) time windows, of 0.8 mM NsC in aqueous buffer (pH 7.5) solutions of 0.1 M Trizma. Emission was collected at indicated wavelengths after excitation at 266 nm.

Our temporal and spectral resolutions show that the fluorescence of sC has three spectral bands having the maxima around 310 (λ_{short}), 360 (λ_{medium}), and 410 nm (λ_{long}) and that the three bands are quite different from one another in temporal behaviors (Fig. 3). Because both Tyr and Trp emit fluorescence from $^1(\pi,\pi^*)$, the λ_{short} band originates from relatively hydrophobic environment and the λ_{long} band does from relatively hydrophilic environment. It is interesting that although the λ_{short} band has the highest energy to be quenched, it decays more slowly than the λ_{medium} band. Tyr residues emitting the short band have tighter environment than those emitting the λ_{medium} band and they cannot undergo internal rotation rapidly. This is the reason why the λ_{short} band is not quenched fastest regardless of its highest energy (vide infra). The λ_{long} band having the lowest energy decays most slowly because the responsible fluorophores do not have any quenching chromophores of low energy. However, it should be mentioned that the time-resolved spectra of Fig. 3 show only approximate temporal behaviors of sC fluorescence because the overall behaviors depend on the initial relative amplitudes and lifetimes of all the decay components present in fluorescence. We can see the details of sC fluorescence kinetic behaviors from Fig. 4.

The protein fluorescence of sC has three temporally distinguishable decay components of 100, 1100, and 3300 ps, designated as fast, medium, and slow components, respectively (Fig. 4 and Table 2). The reason why the λ_{medium} band

TABLE 2 Fluorescence decay constants of NsC at three different wavelengths, extracted from Fig. 4

λ_{em} (nm)	τ_f (ps)	f_f	τ_m (ps)	f_m	τ_s (ps)	f_s
300	100	0.13	1100	0.32	3300	0.55
360	100	0.38	1100	0.22	3300	0.40
420	100	0.12	1100	0.13	3300	0.75

decays fastest superficially in Fig. 3 is that the initial amplitude of the fast component is largest among the three spectral bands. On the other hand, the λ_{long} band decays most slowly as it has the smallest amplitude of the fast component and the largest amplitude of the slow component. We attribute the fast and the medium decay components to energy transfer processes from high-energy Tyr residues at hydrophobic environment to low-energy Tyr residues at hydrophilic environment or to Trp and Tyr^- residues. The slow component arises from the relaxation of low-energy Tyr residues or Trp and Tyr^- residues to their ground state.

The decay kinetics of sC protein fluorescence becomes faster sequentially with stepwise Ca^{2+} removal, although the changes are not substantial (Fig. 5). Table 3 shows that the decay time of only the medium component decreases with Ca^{2+} removal. Tyr residues near both binding sites

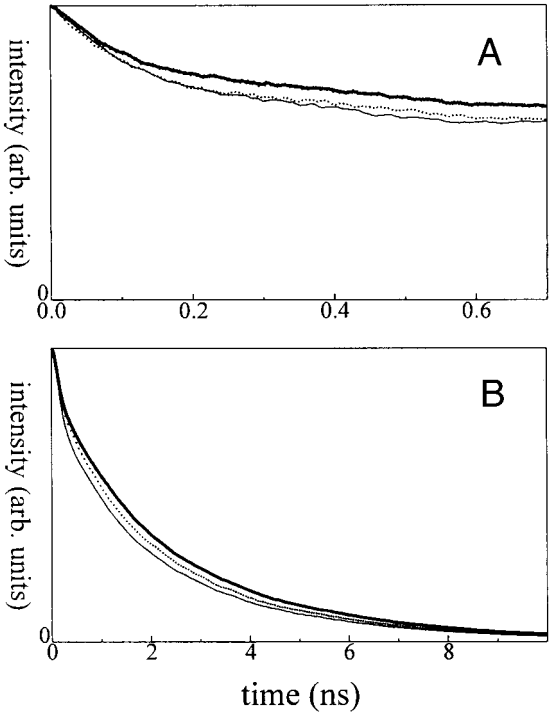

FIGURE 5 Fluorescence kinetic profiles, displayed in short (*a*) and long (*b*) time windows, of NsC (*boldly solid*), dWsC (*dotted*), and dSsC (*thinly solid*) with respective concentrations of 0.8 mM in aqueous buffer (pH 7.5) solutions of 0.1 M Trizma. Fluorescence was monitored at 290+ nm after excitation at 266 nm.

TABLE 3 Ca^{2+}-dependent decay constants of sC fluorescence, extracted from Fig. 5

Sample	τ_f (ps)	f_f	τ_m (ps)	f_m	τ_s (ps)	f_s
NsC	100	0.22	1100	0.23	3300	0.55
dWsC	100	0.25	850	0.23	3300	0.52
dSsC	100	0.25	760	0.27	3300	0.48

TABLE 4 Wavelength-dependent anisotropic decay parameters of NsC fluorescence, extracted from Fig. 6

$\lambda_{monitor}$ (nm)	r_0	ϕ_f (ps)	β_f	ϕ_s (ps)	β_s
300	0.30	410	0.06	12,000	0.24
360	0.13	160	0.12	12,000	0.01
420	0.15	360	0.12	12,000	0.03

have looser environment with Ca^{2+} removal so as to undergo internal rotation and subsequent energy transfer more easily (vide infra). The lifetime of the fast component does not change with Ca^{2+} removal because the Tyr residues responsible for the fast component already have good coupling conditions with Ca^{2+} ions. The lifetime of the slow component does not change obviously as expected. Ca2 removal reduces the decay time by 23%, and Ca1 removal in addition to Ca2 removal reduces the decay time further by 8%. Compared with the strong site, the weak site is more hydrophobic (Lee and Jang, 2000) so that it might have more high-energy Tyr residues nearby. Thus, Ca2 removal reduces the lifetime of the medium component more than Ca1 removal does.

The λ_{short} band among the three protein fluorescence bands of sC shows the largest initial anisotropy and the slowest depolarization kinetics, whereas the λ_{medium} band shows the smallest anisotropy and the fastest kinetics (Fig. 6 and Table 4). The anisotropy of each fluorescence band decays with double rotational correlation times. The fast depolarization time depends on the monitored wavelength strongly, whereas the slow one does not at all. The slow one of 12 ns is ascribed to the overall rotation time of the entire polypeptide because the global rotation time measured from the Trp fluorescence depolarization kinetics of sC is reported to be 11.3 ns (Bayley et al., 1989) and the time is calculated using the Stokes-Einstein relation as 12 ns for the 30 kDa protein of sC (Cantor and Schimmel, 1980). Then the fast component arises from the internal rotation of Tyr and Trp fluorophores with respect to the entire protein motion. As already suggested with Figs. 3 and 4, the fluorophores responsible for the λ_{short} fluorescence band are enclosed by much tighter polypeptide segments than those responsible for the λ_{medium} band. Tyr residues in hydrophilic environment are in looser environment to undergo fast internal rotation than those in hydrophobic environment. This explains why the λ_{medium} fluorescence band decays faster than the λ_{short} band (Figs. 3 and 4).

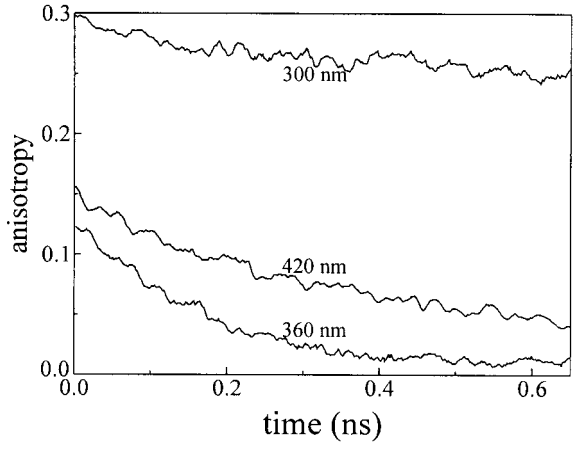

FIGURE 6 Fluorescence depolarization kinetic profiles, excited at 266 nm and collected at shown wavelengths, of 0.8 mM NsC in aqueous buffer (pH 7.5) solutions of 0.1 M Trizma.

Both fast and slow rotational correlation times change significantly with the removal of Ca^{2+} from the weak binding site (Fig. 7 and Table 5). However, none show significant variation with the additional removal of Ca^{2+} from the strong binding site, although we admit that the slow rotational time decreases slightly further. It is interesting that the initial anisotropy does not change at all with Ca^{2+} removal. Very fast internal motions or rapid intermolecular energy transfer processes on a femtosecond-picosecond time scale cause a decrease of the initial anisotropy. Then no change in the initial anisotropy suggests that Ca^{2+} removal does not change rapid processes occurring in a femtosecond-picosecond time scale. The significant reduction of the fast rotational correlation time with Ca2 removal implies that Ca^{2+} binding to the weak binding site causes peptide segments enclosing fluorophores near Ca2 to be less flexible by chelating negatively charged side chains. Because Figs. 1 and 2 have indicated that Ca1 removal also changes the thermal denaturation temperature and secondary structure of sC, Ca1 binding should make peptide segments near Ca1 less flexible as well. No change in the fast rotational time with Ca1 removal rather suggests that the fluorophores of Tyr and Trp residues are not present near Ca1. The decrease of the slow rotational correlation time with Ca^{2+} removal results from decrease in the gyration radius of the global protein. We have shown with Fig. 2 and Table 1 that while the fractions of α-helix and β-sheet decrease, the fraction of random coil increases progressively with Ca^{2+} removal. Then the radius of the gyration decreases apparently with stepwise Ca^{2+} removal, reducing the global rotational time of sC.

CONCLUSION

The polypeptide chain of sC undergoes progressive rearrangement into disorderly and flexible conformation with

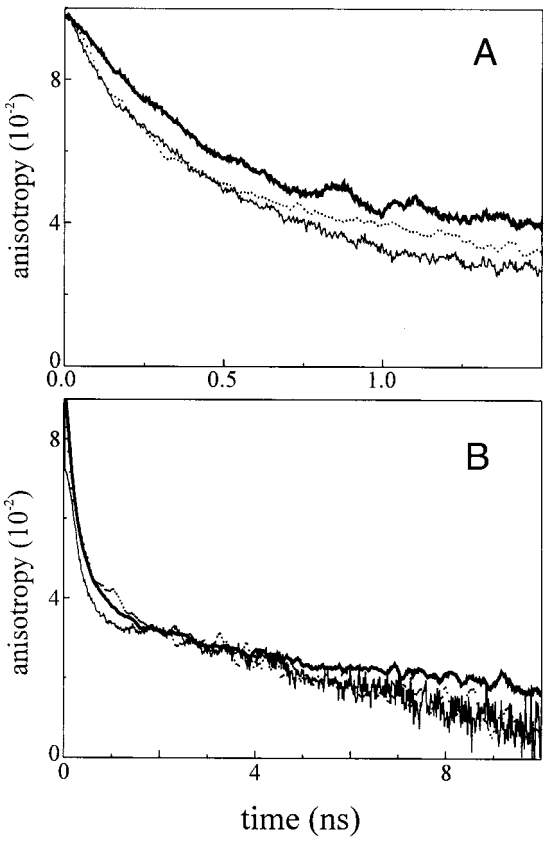

FIGURE 7 Fluorescence depolarization kinetic profiles, displayed in short (*a*) and long (*b*) time windows, of NsC (*boldly solid*), dWsC (*dotted*), and dSsC (*thinly solid*) with respective concentrations of 0.8 mM in aqueous buffer (pH 7.5) solutions of 0.1 M Trizma. Emission was monitored at 290+ nm after excitation at 266 nm.

stepwise Ca^{2+} removal. Thermal denaturation temperature decreases considerably with Ca1 removal, whereas it does slightly with Ca2 removal. On the other hand, the fraction of random coil structure increases significantly with Ca2 removal as well as with Ca1 removal. The near-UV CD hardly changes with Ca2 removal but it does noticeably with Ca1. The enzyme shows three fluorescence decay times of 100, 1100, and 3300 ps. Whereas the fast and the slow do not change noticeably, the medium one decreases progressively with Ca^{2+} removal. The protein has two fluorescence anisotropic decay components. The fast one arises from the internal rotation of Tyr and it decays in 410 ps at 300 nm and in 160 ps at 360 nm. The slow one resulting from the global rotation of sC decays in the time scale of 12 ns. Although both become significantly faster with Ca2 removal, only the slow one becomes slightly faster with further removal of Ca1. Ca^{2+} removal increases the flexibility of sC and decreases the gyration radius of sC significantly. Although Ca1 and Ca2 play different structural roles, both are suggested to be indispensable for the stable structure of sC.

TABLE 5 Ca^{2+}-dependent anisotropic decay parameters of sC fluorescence, extracted from Fig. 7

Sample	r_0	ϕ_f (ps)	β_f	ϕ_s (ps)	β_s
NsC	0.10	340	0.4	12,000	0.6
dWsC	0.10	140	0.4	6100	0.6
dSsC	0.10	140	0.4	5700	0.6

This work was supported by The Center for Molecular Catalysis. We also acknowledge the Korea Research Foundation (KRF-2000–015-DP0913) and the Brain Korea 21 Program, respectively. We thank the Equipment Joint Use Program of the Korea Basic Science Institute.

REFERENCES

Bayley, P. M., J.-M. Janot, and S. R. Martin. 1989. Subtilisin enzymes: a note on time-resolved fluorescence and circular dichroism properties. *FEBS Lett.* 250:389–394.

Bode, W., E. Papamokos, and D. Musil. 1987. The high-resolution X-ray crystal structure of the complex formed between subtilisin Carlsberg and eglin c, an elastase inhibitor from the leech Hirudo medicinalis. *Eur. J. Biochem.* 166:673–692.

Broos, J., A. J. W. G. Visser, J. F. J. Engbersen, W. Verboom, A. van Hoek, and D. N. Reinhoudt. 1995. Flexibility of enzymes suspended in organic solvents probed by time-resolved fluorescence anisotropy: evidence that enzyme activity and enantioselectivity are directly related to enzyme flexibility. *J. Am. Chem. Soc.* 117:12657–12663.

Cantor, C. R., and P. R. Schimmel. 1980. Biophysical Chemistry, part II. Freeman, San Francisco. 460.

Carter, P., and J. A. Wells. 1988. Dissecting the catalytic triad of a serine protease. *Nature.* 332:564–568.

Chang, C. T., C.-S. C. Wu, and J. T. Yang. 1978. Circular dichroic analysis of protein conformation: inclusion of β-turns. *Anal. Biochem.* 91:13–31.

Chatterjee, S., and A. J. Russell. 1993. Kinetic analysis of the mechanism for subtilisin in essentially anhydrous organic solvents. *Enzyme Micro. Technol.* 15:1022–1029.

Chaudhary, A. K., S. V. Kamat, E. J. Beckman, D. Nurok, R. M. Kleyle, P. Hajdu, and A. J. Russell. 1996. Control of subtilisin substrate specificity by solvent engineering in organic solvents and supercritical fluoroform. *J. Am. Chem. Soc.* 118:12891–12901.

Cheng, R. P., S. L. Fisher, and B. Imperiali. 1996. Metallopeptide design: tuning the metal cation affinities with unnatural amino acids and peptide secondary structure. *J. Am. Chem. Soc.* 118:11349–11356.

Fitzpatrick, P. A., D. Ringe, and A. M. Klibanov. 1994. X-ray crystal structure of cross-linked subtilisin Carlsberg in water vs. acetonitrile. *Biochem. Biophys. Res. Commun.* 198:675–681.

Genov, N., B. Filippi, P. Dolashka, K. S. Wilson, and C. Betzel. 1995. Stability of subtilisins and related proteinases (subtilases). *Int. J. Peptide Protein Res.* 45:391–400.

Ghadiri, M. R., and C. Choi. 1990. Secondary structure nucleation in peptides: transition metal ion stabilized α-helices. *J. Am. Chem. Soc.* 112:1630–1632.

Ghadiri, M. R., C. Soares, and C. Choi. 1992. A convergent approach to protein design: metal ion-assisted spontaneous self-assembly of a polypeptide into a triple-helix bundle protein. *J. Am. Chem. Soc.* 114: 825–831.

Grinvald, A., and I. Z. Steinberg. 1976. The fluorescence decay of tryptophan residues in native and denatured proteins. *Biochim. Biophys. Acta.* 427:663–678.

Handel, T. M., S. A. Williams, and W. F. DeGrado. 1993. Metal ion-dependent modulation of the dynamics of a designed protein. *Science.* 261:879–885.

Kidd, R. D., H. P. Yennawar, P. Sears, C.-H. Wong, and G. K. Farber. 1996. A weak calcium binding site in subtilisin BPN′ has a dramatic effect on protein stability. *J. Am. Chem. Soc.* 118:1645–1650.

Kijima, T., S. Yamamoto, and H. Kise. 1994. Fluorescence spectroscopic study of subtilisins as relevant to their catalytic activity in aqueous-organic media. *Bull. Chem. Soc. Jpn.* 67:2819–2824.

Kohn, W. D., C. M. Kay, B. D. Sykes, and R. S. Hodges. 1998. Metal ion induced folding of a de novo designed coiled-coil peptide. *J. Am. Chem. Soc.* 120:1124–1132.

Lakowicz, J. R., B. P. Maliwal, H. Cherek, and A. Balter. 1983. Rotational freedom of tryptophan residues in proteins and peptides. *Biochemistry.* 22:1741–1752.

Lakshmikanth, G. S., and G. Krishnamoorthy. 1999. Solvent-exposed tryptophans probe the dynamics at protein surfaces. *Biophys. J.* 77: 1100–1106.

Lee, S., and D.-J. Jang. 2000. Cation-binding sites of subtilisin Carlsberg probed with Eu(III) luminescence. *Biophys. J.* 79:2171–2177.

Lieberman, M., and T. Sasaki. 1991. Iron(II) organizes a synthetic peptide into three-helix bundles. *J. Am. Chem. Soc.* 113:1470–1471.

McPhalen, C. A., and M. N. G. James. 1988. Structural comparison of two serine proteinase-protein inhibitor complexes: eglin-c-subtilisin Carlsberg and CI-2-subtilisin Novo. *Biochemistry.* 27:6582–6598.

Neidhart, D. J., and G. A. Petsko. 1988. The refined crystal structure of subtilisin Carlsberg at 2.5 Å resolution. *Protein Eng.* 2:271–276.

Nishimoto, E., S. Yamashita, A. G. Szabo, and T. Imoto. 1998. Internal motion of lysozyme studied by time-resolved fluorescence depolarization of tryptophan residues. *Biochemistry.* 37:5599–5607.

Pantoliano, M. W., M. Whitlow, J. F. Wood, S. W. Dodd, K. D. Hardman, M. L. Rollence, and P. N. Bryan. 1989. Large increases in general stability for subtilisin BPN′ through incremental changes in the free energy of unfolding. *Biochemistry.* 28:7205–7213.

Pantoliano, M. W., M. Whitlow, J. F. Wood, M. L. Rollence, B. C. Finzel, G. L. Gilliland, T. L. Poulos, and P. N. Bryan. 1988. The engineering of binding affinity at metal ion binding sites for the stabilization of proteins: subtilisin as a test case. *Biochemistry.* 27:8311–8317.

Ruan, F., Y. Chen, and P. B. Hopkins. 1990. Metal ion enhanced helicity in synthetic peptides containing unnatural, metal-ligating residues. *J. Am. Chem. Soc.* 112:9403–9404.

Saxena, V. P., and D. B. Wetlaufer. 1971. A new basis for interpreting the circular dichroism spectra of proteins. *Proc. Natl. Acad. Sci. USA.* 68:969–972.

Schneider, J. P., and J. W. Kelly. 1995. Synthesis and efficacy of square planar copper complexes designed to nucleate β-sheet structure. *J. Am. Chem. Soc.* 117:2533–2546.

Siezen, R. J., W. M. de Vos, J. A. M. Leunissen, and B. W. Dijkstra. 1991. Homology modelling and protein engineering strategy of subtilases, the family of subtilisin-like serine proteinases. *Protein Eng.* 4:719–737.

Smith, E. L., R. J. Delange, W. H. Evans, M. Landon, and F. S. Markland. 1968. Subtilisin Carlsberg: V. The complete sequence; comparison with subtilisin BPN′: evolutionary relationships. *J. Biol. Chem.* 243: 2184–2191.

Strausberg, S., P. Alexander, L. Wang, T. Gallagher, G. Gilliland, and P. Bryan. 1993. An engineered disulfide cross-link accelerates the refolding rate of calcium-free subtilisin by 850-fold. *Biochemistry.* 32: 10371–10377.

Tian, Z.-Q., and P. A. Bartlett. 1996. Metal coordination as a method for templating peptide conformation. *J. Am. Chem. Soc.* 118:943–949.

Venyaminov, S. Y., and J. T. Yang. 1996. Determination of protein secondary structure. *In* Circular Dichroism and the Conformational Analysis of Biomolecules. G. D. Fasman, editor. Plenum Publishing Corp., New York. 69–107.

Voordouw, G., C. Milo, and R. S. Roche. 1976. Role of bound calcium ions in thermostable, proteolytic enzymes: separation of intrinsic and calcium ion contributions to the kinetic thermal stability. *Biochemistry.* 15: 3716–3724.

Willis, K. J., and A. G. Szabo. 1989. Resolution of tyrosyl and tryptophyl fluorescence emission from subtilisins. *Biochemistry.* 28:4902–4908.

Yang, Z., M. Domach, R. Auger, F. X. Yang, and A. J. Russel. 1996. Polyethylene glycol-induced stabilization of subtilisin. *Enzyme Microbial Technol.* 18:82–89.